EHL TRACTION ANALYSIS OF PERFLUOROPOLYETHER FLUIDS BASED ON BULK MODULUS

T. MAWATARI[(1)], N. OHNO[(1)], B. ZHANG[(1)], M. KANETA[(2)], P. SPERKA[(2)], I. KRUPKA[(2)], M. HARTL[(2)]

[(1)] - mawatari@me.saga-u.ac.jp ; ohno@me.saga-u.ac.jp ; zhang@me.saga-u.ac.jp ;
Saga University, Department of Mechanical Engineering, 840-8502 Saga, Japan
[(2)] - kaneta@fme.vutor.cz ; sperka@fme.vutor.cz ; krupka@fme.vutor.cz ; hartl@fme.vutor.cz ;
Brno University of Technology, Tecknicka 2896/2, 616 69 Brno, Czech Republic

ABSTRACT

Using three kinds of commercial perfluoropolyether (PFPE) fluids, the authors carried out high pressure density test at the pressure up to 1.2 GPa. Tangent bulk modulus and secant bulk modulus of the PFPE fluids were calculated by using the test results. Relationships of these moduli with pressure and temperature were examined. High pressure viscosity of each PFPE fluid was measured and the pressure viscosity coefficients of the PFPE fluids were obtained. In addition, the maximum traction coefficient and the limiting shear stress of each fluid were evaluated from the traction test employing a ball-on-disk testing machine. As a result, it was found that the maximum traction coefficient and the limiting shear stress are closely related to the tangent bulk modulus and the secant bulk modulus, respectively. The significant relationship of the maximum traction coefficient with the molecular packing parameter represented by the product of the pressure viscosity coefficient and the mean Hertzian pressure was also confirmed.

INTRODUCTION

Perfluoropolyether (PFPE) fluids are satisfactorily used in magnetic recording media [1], aerospace industries and satellite instruments [2]. Recently these oils have been introduced as the hydraulic fluids, the high temperature liquid lubricants in the turbine engines [3], and the base oils of high-temperature greases. Although many studies on PFPE have energetically been carried out, the high pressure rheological characteristics and the Elastohydrodynamic lubrication (EHL) traction have not been understood yet. In a number of studies it has been verified that lubricating oils change to the amorphous or the glassy solids at sufficiently high pressure [4]. Especially, taking into account of the significance of the lubricants behavior at high pressure, many theoretical and experimental investigations related to traction drives have been progressed [5].

The authors performed the measurement of EHL traction with a half-toroidal continuously variable transmission (CVT) fluid till the mean Hertzian pressure of 2.0GPa [6]. Rolling speed was up to 30 m/s, and the oil temperature ranged from 313K to 393K. As a result of the experiment, it was found that the maximum traction coefficient is closely related to T_{VE}-T denoting the free volume parameter. Where, T_{VE} and T mean the viscoelastic solid transition temperature and the oil temperature, respectively. However, it is not yet clear from the perspective of mechanical properties of traction fluid. In the previous study, the authors examined each traction property using ten kinds of different lubricating oils. Consequently, it was confirmed that the bulk modulus plays a predominant role in the traction characteristics [7].

The purpose of this paper is to clarify the predominant factor influencing the traction characteristics of PFPE fluid. In the present experiments three kinds of PFPE fluids were employed. High pressure properties of the PFPE fluids were obtained by the high pressure density test and the high pressure viscosity test. Tangent bulk modulus, secant bulk modulus and pressure viscosity coefficient of the PFPE fluids were calculated based on the results of the high pressure tests. The traction properties of the PFPE fluids were measured using a ball-on-disk testing equipment. The results in the traction test and the high pressure properties of the test oils were comprehensively estimated. As a consequence, it was found that the traction properties of the PFPE fluids are closely related to the tangent bulk modulus, the secant bulk modulus, and the molecular packing parameter represented by the product of the pressure viscosity coefficient and the mean Hertzian pressure.

PROPERTIES OF PFPE FLUIDS

In the present study, three kinds of PFPE fluids were employed. These are Fluid K (GPL105), Fluid D (S200) and Fluid F (M25). Their properties are given in Table 1 [8] and chemical formulas are shown below the table.

HIGH PRESSURE RHEOLOGY

Bulk modulus and phase diagram

The high-pressure density measurement of the test fluids was performed using the high-pressure densitometer shown in Fig. 1 [9]. Two milliliters of the test fluid was poured into the test machine and pressure was applied to the upper plunger by a hydraulic power unit. A load cell was placed below the lower plunger and used to record total load acting on the plunger. The chamber pressure p is given by $(W_1+W_2)/2A$. Where, W_1 is the applied load by the hydraulic power unit, W_2 is the detecting load of the load cell, and A is the area of the bore in the high pressure chamber. The volume of lubricant in the chamber corresponding to a pressure is determined from the displacement of the upper plunger by using a linear gauge. The lubricant volume at high pressure was corrected taking account of the elastic deformation of upper plunger, lower plunger and bore area. Lubricant density was calculated from the lubricant volume measured at test temperature and pressure.

Table 1. Properties of PFPE fluids.

Fluid	ρ, g/mL	ν, mm²/s		VI	M
	288 K	313 K	373 K		g/mol
K (GPL105)	1.910	168.1	18.24	121	4700
D (S200)	1.886	194.6	34.72	227	8400
F (M25)	1.847	141.7	41.88	334	9500

Chemical formulas:

Fluid K (GPL105): $F[C(CF_3)FCF_2O]_nCF_2CF_3$

Fluid D (S200): $F(CF_2CF_2CF_2O)_nCF_2CF_3$

Fluid F (M25): $CF_3[(OCF_2CF_2)_p(OCF_2)_q]OCF_3$

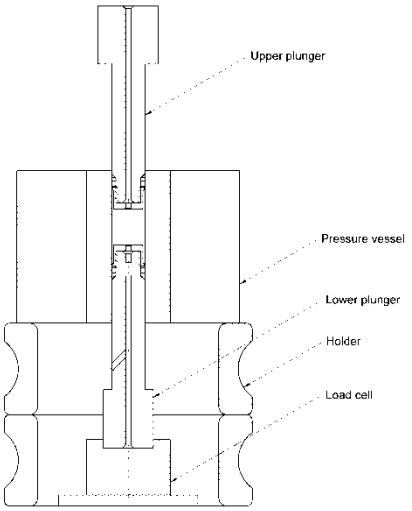

Figure 1. High-pressure densitometer.

One of the basic equations for the solidification of oils is the equation of volumetric change used in the strength of materials. The volumetric strain ε is defined as the ratio of the decrease in volume to the original volume [10]:

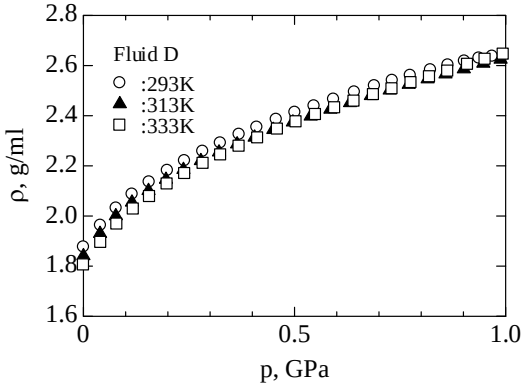

Figure 2. Density-pressure relation of fluid D

$$\varepsilon = \frac{dV}{V} = \left(-\frac{\partial \ln \rho}{\partial p}\right)_T dp + \left(-\frac{\partial \ln \rho}{\partial T}\right)_p dT$$
$$= \left(-\frac{1}{K_T}\right) dp + 3\delta dT \qquad \text{(Eq. 1)}$$

The symbols of V, ρ, T, K_T and δ in above equation represent the volume, the density, the temperature, the tangent bulk modulus and the coefficient of thermal expansion, respectively.

The relations between density and pressure in the Fluid D obtained by the high pressure density test are shown in Fig. 2. Test temperatures are 293K, 313K and 333K.

Differentiating the pressure-density curve, the tangent bulk modulus $K_T = (d\ln\rho/dp)^{-1}$ was calculated. Figure 3 shows the relation between the tangent bulk modulus and the pressure. Secant bulk modulus $K_S = (\rho/(\rho-\rho_0))p$ is also shown in the figure. Where ρ_0 is the density at atmospheric pressure. The viscoelastic solid transition point p_{VE} of fluid D is obvious from the abrupt change of dK_T/dp in Fig. 3 (b). The viscoelastic solid transition pressures were 0.73GPa and 0.90GPa at the test temperatures of 293 K and 313 K, respectively.

The viscoelastic solid transition temperature T_{VE} is expressed as the function of pressure and temperature, and is calculated by the following equation.

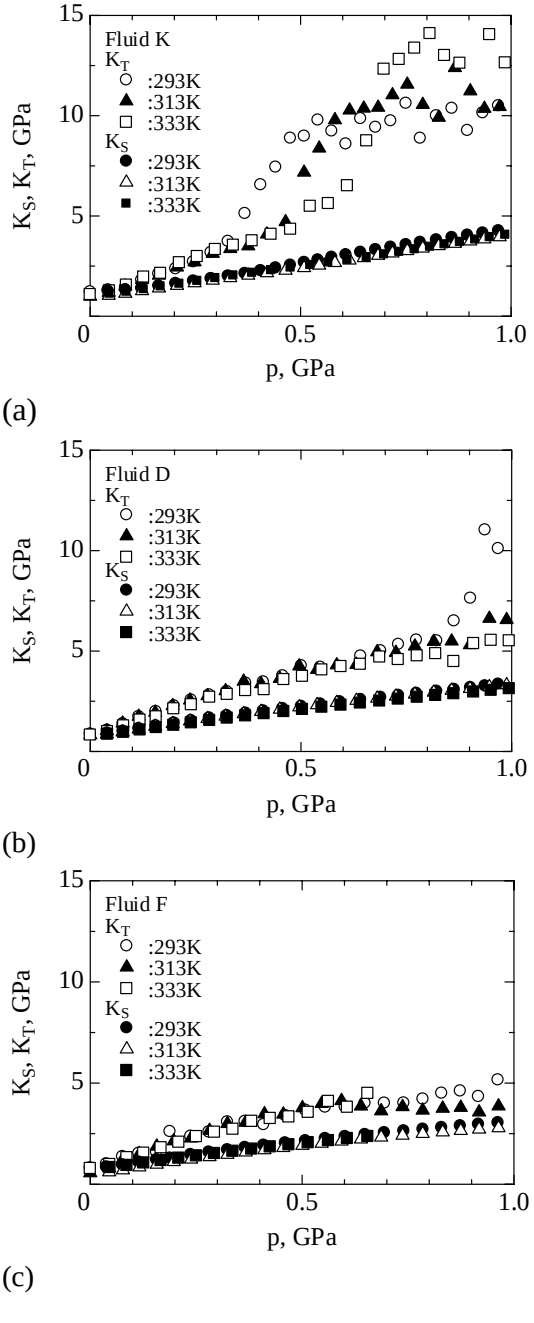

Figure 3. Tangent bulk modulus K_T and secant bulk modulus K_S relationships with pressure p, (a) of Fluid K, (b) of Fluid D and (c) of Fluid F.

Table 2. Rheological parameters of PFPE fluids.

Fluid name	T_{VE0}, K	A_1, K	A_2, GPa^{-1}	B_1	B_2	C_1	C_2
K	209	222.8	1.562	10.33	37.2	-14.74	21.54
D	167	287.8	0.729	12.38	102.36	0.37	7.96
F	147	325.7	0.583	10.93	76.75	8.41	2.51

$$T_{VE} = T_{VE0} + A_1 \ln(1 + A_2 p) \quad \text{(Eq. 2)}$$

Where A_1 and A_2 represent the parameters depending on fluid properties. These parameters are listed in Table 2. The appearance temperature of the photoelastic effect caused by the liquid nitrogen gas cooling was regarded as the viscoelastic solid transition temperature T_{VE0} at atmospheric pressure. T_{VE0} are given in Table 2.

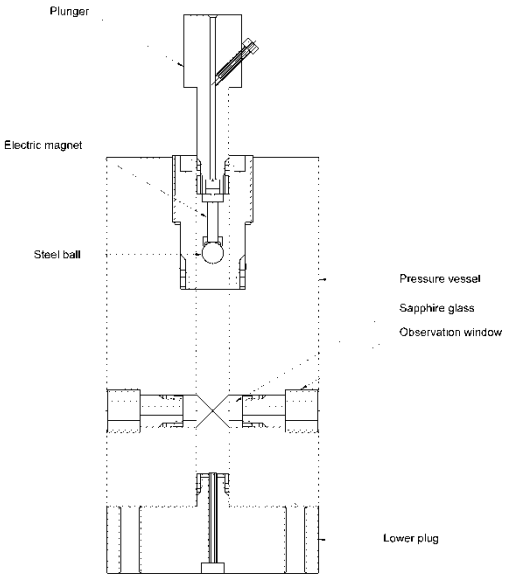

Figure 4. High pressure viscometer.

Viscosity-pressure-temperature relation

A high pressure falling body viscometer was used to measure high pressure viscosity at the pressure of 0.4 GPa or less. When test temperatures ranged from 293 K to 313 K, the absolute viscosity η showed value less than 10^3 Pa·s. The schematic diagram of the falling ball viscometer is shown in Fig. 4 [9]. A solid body with higher density than a test liquid falls slowly through the tube filled with the liquid. A steel ball with the diameter of 7.94 mm dropped down into the viscometer filled with oil, and then passed through the sapphire observation window with the diameter of 3 mm. The time for the falling ball to cross the sapphire window was measured by a sensor. In order to calibrate the viscometer, the high pressure viscosity of the castor oil [9] was compared with those measured by Sargent [11], and it was confirmed that these agree well with each other.

Figure 5 shows the high pressure viscosity of fluid D. The values of the Barus pressure-viscosity coefficient α (GPa^{-1}) were calculated using the least squares method. The variations of the pressure-viscosity coefficient α can be described by the following equation.

$$\alpha = C_1 + C_2 \log_{10} \nu \quad \text{(Eq. 3)}$$

Where ν represents the kinematic viscosity (mm^2/s) at atmospheric pressure. The parameters of C_1 and C_2 are shown in Table 2.

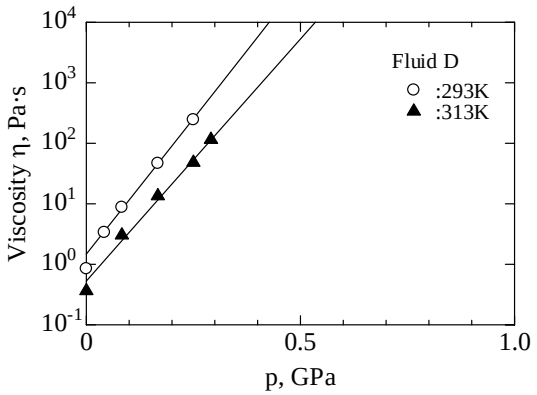

Figure 5. Predicted and observed values of high pressure viscosity of fluid D.

The authors proposed a very useful viscosity-pressure-temperature correlation based on the free volume and the phase diagram [10]. The relational equation is given below:

$$\log_{10} \eta = 7 - \frac{B_1 (T - T_{VE})(T_{VE0}/T_{VE})}{B_2 + (T - T_{VE})(T_{VE0}/T_{VE})} \quad \text{(Eq. 4)}$$

Results of regression analysis of the viscosity data are described in Table 2. Solid lines in Fig. 5 are the theoretical curves drawn by Eq. (4), and the predicting values match well with the experimental results.

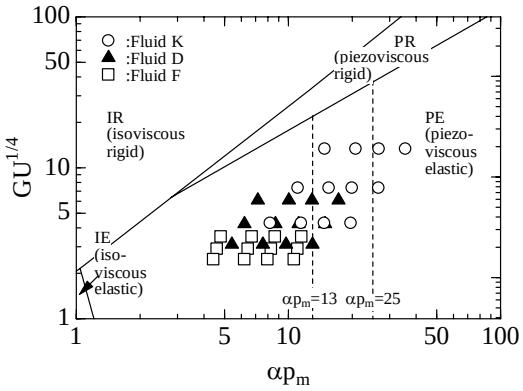

Figure 6. Experimental points in liquid/solid transition lubrication diagram.

EHL TRACTION MEASUREMENT

Experimental method

The traction properties of the PFPE fluids were measured by means of a mini traction machine MTM (PCS Instruments, London, UK). In the testing machine, a rolling sliding lubricated contact is formed by the combination of steel ball and polished flat steel disc. The diameters of the steel ball and the flat steel disk are 19.05 mm and 46 mm respectively. The ball shaft is tilted so that spin becomes nominally zero in point contact. The ball and the disc are driven by independent DC motors.

The ball and the discs were made of AISI52100 bearing steel (Young's modulus E=210 GPa, Poisson's ratio ν=0.3). The contact surfaces of ball and disk were finished to roughness of Rq=10-13 nm and 25-30 nm (Rq: root mean square roughness of the profile according to ISO 4287-1997 or JIS B 0601-2001) [12]. The loads of 4.2 N, 12.4 N, 26.4 N and 62.6 N were applied in point contact. The corresponding maximum Hertzian pressures P_H to the applied loads are 0.5 GPa, 0.7 GPa, 0.9 GPa and 1.2 GPa, respectively. The traction testing machine can be performed at the entrainment speed of 0.05 m/s or more. The lowest entrainment speed of 0.05 m/s was selected for reducing the shear heating effect as possible. In the traction test, the slide roll ratio was increased under the constant entrainment speed. The ambient temperature of each traction test was fixed at 293 K, 313 K or 333 K, respectively. From the test results, the relation between the traction coefficient and slide roll ratio was examined.

Results of traction measurement

Regarding the traction force measurement and observation, it is very important that the experiments are carried out in the full EHL regime where the traction components never depend on boundary lubrication. Hamrock-Dowson diagram [13] is commonly used for identification of the lubrication regime in point contact. Lubrication regimes in the diagram are divided into four regimes, namely, isoviscous-rigid (IR) regime, piezoviscous-rigid (PR) regime, isoviscous-elastic (IE) regime and piezoviscous-elastic (PE) regime. The authors [14] previously concluded that the most suited method for estimating the solidified film thickness in EHL contact is to use the liquid/solid transition lubrication diagram. The transition lubrication diagram is composed by combining Greenwood diagram [15]. That is, abscissa and ordinate are represented by αp_m and $GU^{1/4}$. In the terms constituting the abscissa and ordinate parameters, p_m, G and U mean average pressure, dimensionless material parameter and dimensionless speed parameter. The liquid/solid transition condition is depending on αp_m [16]. When αp_m is 13, the phase transition between the liquid and the viscoelastic solid occurs. In addition, the phase transition between viscoelastic solid and elastic-plastic solid arises at αp_m=25. The experimental ranges at the elliptical parameter of k=1 are plotted in Fig. 6. In the present traction tests, the lubricants state ranges from liquid to elastic-plastic solid. Besides, all tests are included in the PE regime and so the minimum film thickness can be calculated by the EHL formula of Hamrock-Dowson. Film parameter Λ, that is, the ratio of the minimum film thickness to the composite roughness spreads in the ranges from 1 to 40.

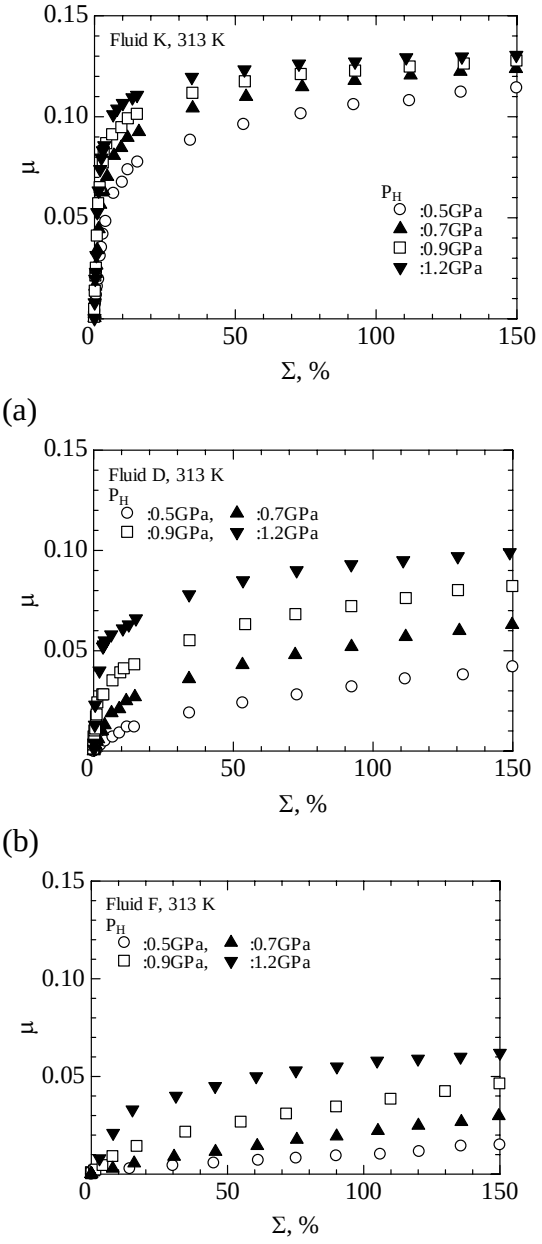

Figure 7. Traction curves (a) of Fluid K, (b) of Fluid D and (c) of Fluid F obtained by traction test at temperature of 313 K and entrainment speed of 0.05 m/s.

Figure 7 shows the traction test results at the ambient temperature of 313 K. As shown in the figure, the traction coefficient changed depending on the slide roll ratio. First, the traction coefficient showed the tendency to increase linearly with increase in the slide roll ratio. And then, in many cases, the nonlinear relation between them was observed by further increase in the slide roll ratio. In addition, it was found that the traction coefficient and its maximum value are different depending on the Hertzian pressure and the test fluids.

Table 3. αp, maximum traction coefficient μ_{max}, limiting shear stress τ_{max}, tangent bulk modulus K_T and secant bulk modulus K_S at 313 K.

Fluid name	P_H, GPa	αp_m	μ_{max}	τ_{max}, GPa	K_T, GPa	K_S, GPa
K	0.5	11.2	0.114	0.038	3.4	1.9
	0.7	15.6	0.124	0.058	4.8	2.3
	0.9	20.1	0.128	0.077	10.0	2.7
	1.2	26.8	0.131	0.104	10.4	3.4
D	0.5	6.2	0.042	0.014	3.2	1.8
	0.7	8.7	0.063	0.029	3.9	2.1
	0.9	11.2	0.082	0.049	4.3	2.5
	1.2	14.9	0.099	0.079	5.4	2.9
F	0.5	4.6	0.015	0.005	3.0	1.5
	0.7	6.4	0.030	0.014	3.5	1.8
	0.9	8.3	0.046	0.028	4.1	2.1
	1.2	11.0	0.062	0.049	3.7	2.5

The authors [16] previously pointed out that the product of the pressure viscosity coefficient α and the mean Hertzian pressure p_m is closely related to the oil molecular packing states. Maximum value of each traction curve shown in Fig. 7 was treated as maximum traction coefficient μ_{max}. Limiting shear stress τ_{max} was calculated by product of the mean Hertzian pressure p_m and the maximum traction coefficient μ_{max}. The tangent bulk modulus K_T and the secant bulk modulus K_S at specific mean Hertzian pressure can be obtained from Fig. 3. The values of αp_m, μ_{max}, τ_{max}, K_T and K_S at each P_H are shown in Table 3.

DISCUSSIONS

The relation between the maximum traction coefficient μ_{max} and the molecular packing parameter αp_m is shown in Fig. 8. The maximum traction coefficients are the values obtained by the traction tests at the temperature range from 293 K to 333 K. As the molecular packing parameter αp_m becomes large, the maximum traction coefficient μ_{max} tends to increase. However,

the increase rate of the traction coefficient is different depending on the phase state of each PFPE fluid. When the molecular packing parameter αp_m is less than 13, the test fluid is in liquid state, and the maximum traction coefficient μ_{max} shows the rapid increase with rise in αp_m. In the case of the molecular packing parameter αp_m of 13 or more, the test fluid shows solid state, and the increase rate becomes moderate compared with those in αp_m of less than 13.

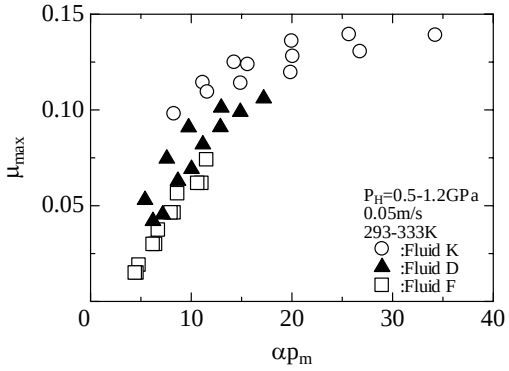

Figure 8. Relation between maximum traction coefficient μ_{max} and molecular packing parameter αp_m.

Figure 9 shows the relation between the maximum traction coefficient μ_{max} and the tangent bulk modulus K_T. Although the maximum traction coefficient of the fluid K with high tangent bulk modulus shows larger value than the fluids D and F with lower tangent bulk modulus, it was found that the same significant correlation as that between αp_m and μ_{max} exists between K_T and μ_{max}.

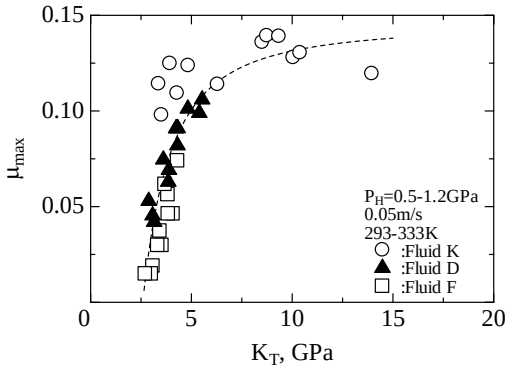

Figure 9. Relation between maximum traction coefficient μ_{max} and tangent bulk modulus K_T.

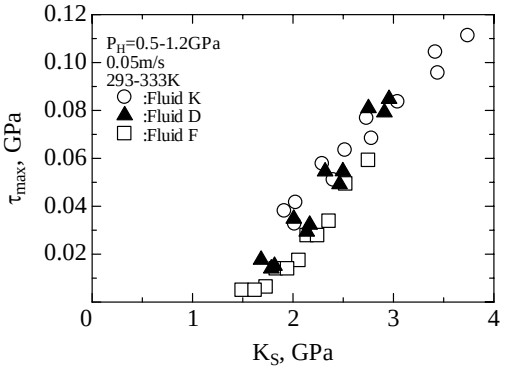

Figure 10. Relation between limiting shear stress τ_{max} and secant bulk modulus K_S.

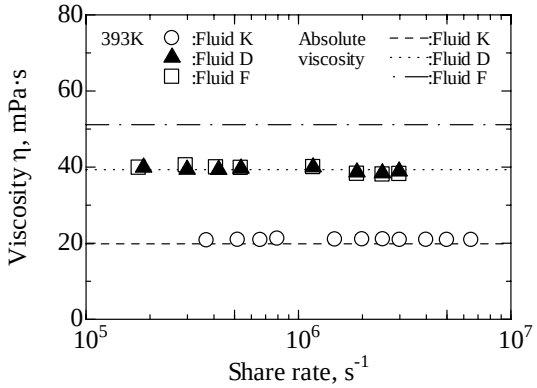

Figure 11. Fluid viscosity at high shear rates.

Figure 10 shows the relation between the limiting shear stress τ_{max} and the secant bulk modulus K_S. There is also a remarkable interrelation between the limiting shear stress τ_{max} and the secant bulk modulus K_S. Namely, independent of the kinds of PFPE fluid, the limiting shear stress τ_{max} shows the tendency to increase linearly with increase in the secant bulk modulus K_S. Considering the correlations obtained from Figs 8, 9 and 10, it was found that a significant physical properties estimating the traction behavior of the PFPE fluids are the molecular packing parameter αp_m, the tangent bulk modulus K_T and the secant bulk modulus K_S.

Figure 11 shows the values of fluid viscosity under high shear rate conditions. In order to measure the viscosity at high shear rate in the range of 1.8×10^5 s^{-1} to 6.5×10^6 s^{-1}, the ultra shear viscometer of PCS instruments was used. The measuring temperature was fixed at 393 K. Marks in the figure are corresponded to test results. The broken line, dotted line and chain line indicate the viscosity values of

fluid K, fluid D and fluid F, respectively. As shown in this figure, each viscosity was almost constant independent of the shear rate. In the case of fluid K and fluid D, each viscosity at the high shear rates is almost the same as the absolute viscosity. On the other hand, it was found that the viscosity of fluid F clearly decreases in comparison with the absolute viscosity.

All traction tests in the fluid F were performed in the liquid region with the molecular packing parameter αp_m of less than 13. As shown in Figs 7, 8, 9 and 10, the traction coefficient μ and the maximum shear stress τ_{max} became lower than the fluids K and D. Therefore, it was suggested that such traction property in the fluid F is caused by the viscosity decline at the EHL region exposed to the relatively high shear rates. Furthermore, in the case of fluid F, it was found that both the tangent bulk modulus K_T and the secant bulk modulus K_S closely related to the molecular structure become smaller than the other fluids.

CONCLUSIONS

Using three kinds of PFPE fluids, the high pressure density and viscosity tests was performed. The tangent bulk modulus K_T, the secant bulk modulus K_S and the pressure viscosity coefficient α in the PFPE fluids were obtained based on the results in the high pressure tests. The traction coefficients μ of the PFPE fluids were also measured by means of a ball-on-disk test equipment, and the values of the limiting shear stress τ_{max} were calculated. In addition the relations between the high pressure properties and the traction properties in the PFPE fluids were comprehensively examined. Consequently, the following conclusions were derived.

i) The maximum traction coefficient μ_{max} showed the tendency to increase with increase in the molecular packing parameter αp_m. In addition, the increase rate varied depending on the phase state of PFPE fluid.

ii) The same significant correlation as that between αp_m and μ_{max} were also found between the tangent bulk modulus K_T and the maximum traction coefficient μ_{max}.

iii) Independent of the kinds of PFPE fluid, there was a remarkable interrelation between the limiting shear stress τ_{max} and the secant bulk modulus K_S.

iv) The bulk modulus is affected by the lubricant molecular structure and the molecular packing state. The higher bulk modulus means the denser molecular packing state. The state of the molecular packing governs the shear resistance, namely the traction properties. Therefore, the traction characteristics of test fluids can be estimated using the bulk modulus and the molecular packing parameter.

ACKNOWLEDGEMENT

The authors would like to express their sincere thanks to Dr. K. Matsumoto, Honda R&D Co. Ltd., Japan for the enormous cooperation of the fluid viscosity measurements at high shear rates.

REFERENCE

1. Bhusan, B., 1990, “Tribology and Mechanics of Magnetic Storage Devices, Springer,” New York.
2. Jones, Jr., W. R., 1995, “Properties of Perfluoropolyethers for Space Applications,” STLE Trib. Trans, 38 (3), pp. 557-564.
3. Liang, J. C., Holmick, L. S., 1996, “Tribochemistry of a PFPAE Fluid on M-50 Surfaces by FTIR Spectroscopy,” STLE Trib. Trans, 39 (3), pp. 705-709.
4. Alsaad, M., Bair, S., Sanborn, D. M., Winer, W. O., 1978, “Glass Transition in Lubricants: Its Relation to Elastohydrodynamic Lubrication (EHD),” ASME J. Lubr. Technol., 100 (3), pp. 404-417.

5. Evans, C. R., Johnson, K. L., 1986, “Regimes of Traction in Elastohydrodynamic Lubrication,” Proc. IMech E, 200 (C5), pp.313-324.
6. Ohno, N., Achiha, H., Natsumeda, S., Aihara, S., Hirano, F., 1999, “High Pressure Rheology and Traction Characteristics of Traction Oil,” Journal of Japanese Society of Tribologists, 44 (12), pp. 965-972.
7. Ohno, N., Rahman, MD. Z., Kakuda, K., 2005, “Bulk Modulus of Lubricating Oils as Predominant Factor Affecting Tractional Behavior in High - Pressure Elastohydrodynamic Contacts,” STLE Trib. Trans, 48, pp.165-190.
8. Ohno, N., Rahman, MD. Z., Yamada, S., Komiya, H., 2009, “Effect of Perfluoropolyether Fluids on Life of Thrust Ball Bearings,” STLE Trib. Trans, 52, pp.492-450.
9. Mawatari, T., Fukuda, R., Mori, H., Mia, S., Ohno, N., 2013, “High Pressure Rheology of Environmentally Friendly Vegetable Oils,” Tribology Letters, 51 (2), pp.273-280.
10. Ohno, N., Hirano, F., 2001, “High Pressure Rheology Analysis of traction Oils Based on Free Volume Measurement,” Lubr. Eng., 57 (7), pp.16-22.
11. Sargent, Jr., L. B., 1995, “Significance of Viscosity Studies of Fluid Lubricants at High Pressure,” Lubr. Eng., July-August, pp.249-254.
12. Muller, M., Topolovec-Miklozic, K., Dardin, A., Spikes, H. A., 2006, “The Design of Boundary Film-Formation PMA Viscosity Modifiers,” STLE Trib. Trans., 49, pp.225-232.
13. Hamrock, B. J., Dowson, D., 1981, “Ball Bearing Lubrication,” Wiley and Sons, Inc., New York.
14. Ohno, N., Kuwano, N., Hirano, F., 1994, “Diagrams for Estimation of the Solidified Film Thickness at High Pressure EHD Contacts,” Dissipative Processes in Tribology, Eds, D. Dowson, C.M. Taylor, T.H.C. Childs, M. Godet, and G. Dalmaz, Elsevier, Amsterdam, pp.507-518.
15. Greenwood, J. A., 1988, “Film Thickness in Circular Elastohydrodynamic Contacts,” Proc. IMech E, 202 (C1), pp.11-17.
16. Ohno, N., Hattori, N., Kuwano, N., Hirano, F., 1988, “Some Observations on the Relationship between Rheological Properties of Lubricants at High Pressure and Regimes of Traction (Part 1) – The Rheological Properties of Lubricants at High Pressure - ,” Journal of Japan Society of Lubrication Engineers, 33 (12), pp.922-928.

The paper was presented at
NORDTRIB2014, Aarhus, Denmark.